 ©2005 Kvantovaya Elektronika and Turpion Ltd

PACS numbers: 42.55.Lt; 42.60.Lh
DOI: 10.1070/QE2005v035n07ABEH008959

Spatial homogeneity criteria for active media of cataphoresis repetitively pulsed metal vapour lasers

G.D. Chebotarev, O.O. Prutsakov, E.L. Latush

***Abstract*. The formation of the transverse distribution of the metal vapour concentration in repetitively pulsed lasers is analysed. The criterion for the homogeneity of this distribution is found. The optimal conditions for excitation of the active media of cataphoresis repetitively pulsed metal vapour lasers are determined under which a high degree of both longitudinal and transverse homogeneity is achieved.**

Keywords: *metal vapour lasers, repetitively pulsed discharge, thermal diffusion.*

1. Introduction

Cataphoresis has been long successfully used in cw ion metal vapour lasers (MVLs) to produce a homogeneous distribution of metal vapours along the active medium [1, 2]. The most popular laser of this type is a He – Cd laser (441.6 and 325 nm). Because of the simplicity and reliability of its design, which is only slightly more complex than that of a He – Ne laser, and convenience in operation, the He – Cd laser is the most commercially successful laser among MVLs.

We used for the first time [3 – 5] the cataphoresis method of introducing vapours into active media of repetitively pulsed MVLs, in particular, a 533.7/537.8-nm He – Cd and a 430.5-nm He – Sr lasers and demonstrated the outlook for using cataphoresis in repetitively pulsed lasers. Thus, we obtained the record specific average output power $P_{\rm av}^{\rm sp} = 277$ mW cm^{-3} for a small He – Sr laser with a discharge channel diameter of 3 mm and the active medium of length 26 cm upon cataphoresis transportation of the strontium vapour.

We estimated [6, 7] the transportation rate of metal vapours in a repetitively pulsed regime and the time of establishment of the longitudinal distribution of the concentration of metal vapours and obtained the criterion for its homogeneity. The aim of this paper is to study the formation of the transverse distribution of the concentration of metal vapours due to radial cataphoresis and thermal diffusion in a repetitively pulsed discharge, to determine the criterion for the homogeneity of this distribution, and to find the optimal conditions for excitation of the active media of cataphoresis repetitively pulsed MVLs that would provide their high homogeneity.

G.D. Chebotarev, O.O. Prutsakov, E.L. Latush Department of Physics, Rostov State University, ul. Zorge 5, 344090 Rostov-on-Don, Russia; e-mail: latussh@phys.rsu.ru

Received 31 March 2005
Kvantovaya Elektronika **35** (7) 598 – 604 (2005)
Translated by M.N. Sapozhnikov

2. Transverse distribution of metal vapours

The radial distribution of the concentration of particles in a repetitively pulsed discharge evolves during the entire interpulse period. Let us find the average radial distribution of the metal vapour concentration established for the interpulse period. This distribution, as the longitudinal distribution, is established not at once but after some time, which in longitudinal-discharge-excited lasers is much shorter than the establishment time of the longitudinal distribution because the diameter $2R$ of a gas-discharge channel is much smaller than its length. Therefore, we will assume that the radial distributions of plasma parameters averaged over the interpulse period quasi-stationary adjust to the longitudinal distributions. We will consider the concentration $N_{\rm M}(r)$ of metal atoms, concentration $N_{\rm M^+}(r)$ of metal ions, and the gas temperature $T_{\rm g}(r)$ averaged over the interpulse period. The following simplifying assumptions will be used: (i) a metal is predominantly ionised, i.e., $N_{\rm M^+}(r) = N_{\rm e}$, where $N_{\rm e}$ is the electron concentration; (ii) energy is introduced into a discharge uniformly along its radius; (iii) the current pulse duration $\tau_{\rm i}$ is much shorter than the interpulse period T; (iv) the diffusion coefficients of metal atoms and ions are identical: $D_{\rm M} = D_{\rm M^+} = D$. These assumptions are well fulfilled under optimal lasing conditions in repetitively pulsed MVLs.

Taking the latter assumption into account, the diffusion equations for $N_{\rm M}(r)$ and $N_{\rm M^+}(r)$ have the form

$$\frac{1}{r}\frac{\rm d}{{\rm d}r}\left[r\frac{D}{T_{\rm g}}\frac{\rm d}{{\rm d}r}(N_{\rm M}T_{\rm g})\right] = Q, \tag{1}$$

$$\frac{1}{r}\frac{\rm d}{{\rm d}r}\left[r\frac{D_{\rm a}}{T_{\rm g}}\frac{\rm d}{{\rm d}r}(N_{\rm M^+}T_{\rm g})\right] = -Q, \tag{2}$$

where $D_{\rm a}$ is the ambipolar diffusion coefficient, which is related to D by the expression

$$D_{\rm a} = D\left(1 + \frac{T_{\rm e}}{T_{\rm g}}\right). \tag{3}$$

The electron temperature $T_{\rm e}$ in (3) also should be considered as averaged over the interpulse period. The radial distribution of $T_{\rm e}$ during the interpulse period approximately repeats the distribution of $T_{\rm g}$, so that the parameter

$$\xi = 1 + \frac{T_e}{T_g} \tag{4}$$

can be considered independent of r.

The function Q of the radial coordinate r has the form

$$Q = \alpha N_M N_e - \beta N_{M^+} N_e^2, \tag{5}$$

where α and β are the interpulse-period-averaged rate constants of ionisation of metal atoms and three-body recombination of metal ions, respectively.

The diffusion coefficient D is a function of the gas temperature and the buffer gas concentration N_b. In most cases, it has the form

$$D = a\frac{\sqrt{T_g}}{N_b}, \tag{6}$$

where a is a constant depending on a particular metal–buffer gas mixture (for strontium in helium, $a = 9.44 \times 10^{19}$ cm^{-1} s^{-1} eV$^{-0.5}$ [8]). Hereafter, T_g is measured in electron-volts.

Let us introduce for convenience the dimensionless spatial variable

$$x = \frac{r}{R} \tag{7}$$

and normalise the concentration of particles to the metal vapour concentration $N_{M,w}$ near the tube walls:

$$n_M = \frac{N_M(r)}{N_{M,w}},\ n_{M^+} = \frac{N_{M^+}(r)}{N_{M,w}},\ n_b = \frac{N_b(r)}{N_{M,w}},\ n_e = \frac{N_e(r)}{N_{M,w}}. \tag{8}$$

Taking (6)–(8) into account, Eqns (1) and (2) can be rewritten in the form

$$\frac{1}{x}\frac{d}{dx}\left[x\frac{1}{n_b\sqrt{T_g}}\frac{d}{dx}(n_M T_g)\right] = \frac{QR^2}{a}, \tag{9}$$

$$\xi\frac{1}{x}\frac{d}{dx}\left[x\frac{1}{n_b\sqrt{T_g}}\frac{d}{dx}(n_{M^+} T_g)\right] = -\frac{QR^2}{a}. \tag{10}$$

The solutions of Eqns (9) and (10) should satisfy the boundary conditions

$$\frac{dn_M(0)}{dx} = \frac{dn_{M^+}(0)}{dx} = 0,\ n_M(1) = 1,\ \ n_{M^+}(1) = 0. \tag{11}$$

By integrating Eqn (9), we obtain

$$x\frac{1}{n_b\sqrt{T_g}}\frac{d}{dx}(n_M T_g) = \frac{R^2}{a}\int Q(x)x\,dx + C_1; \tag{12}$$

It follows from boundary condition (11) for n_M on the axis (for $x = 0$) that $C_1 = 0$. By integrating both parts of Eqn (12), we obtain

$$n_M T_g = \frac{R^2}{a}\int\left[\frac{n_b\sqrt{T_g}}{x}\int Q(x)x\,dx\right]dx + C_2. \tag{13}$$

The integration of Eqn (10) gives

$$\xi n_{M^+} T_g = -\frac{R^2}{a}\int\left[\frac{n_b\sqrt{T_g}}{x}\int Q(x)x\,dx\right]dx + C_2^*. \tag{14}$$

By adding (13) and (14), we obtain

$$(n_M + \xi n_{M^+})T_g = C_2 + C_2^*. \tag{15}$$

It follows from boundary conditions (11) on the wall (for $x = 1$) that

$$C_2 + C_2^* = T_w, \tag{16}$$

where T_w is the tube wall temperature.

By using (15) and (16), we obtain the radial distribution of the concentration of metal atoms in the form

$$n_M(x) = \frac{T_w}{T_g(x)} - \xi n_{M^+}(x). \tag{17}$$

The first term in the right-hand side of Eqn (17) is the radial profile resulting from the inhomogeneous radial distribution of the gas temperature and formed due to thermal diffusion; we denote it as

$$n_M^{(T)}(x) = \frac{T_w}{T_g(x)}. \tag{18}$$

In the case of the homogeneous radial distribution of T_g, expression (17) is the radial profile $n_M(x)$ formed due to radial cataphoresis:

$$n_M^{(D)}(x) = 1 - \xi n_{M^+}(x). \tag{19}$$

Finally, expression (17) can be written in the form

$$n_M(x) = n_M^{(T)}(x) + n_M^{(D)}(x) - 1. \tag{20}$$

2.1 Radial cataphoresis

The radial profile of the concentration of metal atoms caused by radial cataphoresis has form (19). Let us assume that the radial profile $n_{M^+}(x)$ of ions is a parabola with downward branches [9]:

$$n_{M^+}(x) = n_{M^+}(0)(1 - x^2). \tag{21}$$

By replacing $n_{M^+}(0)$ in (21) with $n_e(0)$ (the first simplifying assumption) and substituting the result into (19), we obtain

$$n_M^{(D)}(x) = 1 - \xi n_e(0)(1 - x^2). \tag{22}$$

The time dependence of the electron concentration in afterglow is determined by three-body recombination and ambipolar diffusion. This equation on the tube axis can be written in the form

$$\frac{dN_e}{dt}(0,t) = -\beta N_e^3(0,t) - \gamma_a N_e(0,t), \tag{23}$$

where

$$\gamma_a = \xi\gamma = \xi\frac{6D}{R^2} \tag{24}$$

is the frequency of ambipolar diffusion. The three-body recombination coefficient β is defined by the expression [10]

$$\beta = 3.192 \times 10^{-27} T_e^{-4.5}. \tag{25}$$

By assuming that afterglow begins at the instant $t = 0$ (the third simplifying assumption), we obtain $N_e(0,0) = N_{e,max}(0)$. Then, the solution of Eqn (23) will have the form

$$N_e(0,t)=\left[\left(\frac{1}{N_{e,max}^2(0)}+\frac{\beta}{\gamma_a}\right)\exp(2\gamma_a t)-\frac{\beta}{\gamma_a}\right]^{-1/2}. \quad (26)$$

By averaging $N_e(0,t)$ for the interpulse period T, we obtain

$$\langle N_e(0,t)\rangle=\frac{1}{T}\int_0^T N_e(0,t)\mathrm{d}t$$

$$=\frac{f}{(\gamma_a\beta)^{1/2}}\left\{\arctan\left[\left(\frac{\gamma_a}{\beta N_{e,max}^2(0)}+1\right)\exp\left(\frac{2\gamma_a}{f}\right)-1\right]^{1/2}\right.$$

$$\left.-\arctan\left[\frac{\gamma_a}{\beta N_{e,max}^2(0)}\right]^{1/2}\right\}, \quad (27)$$

where $f=1/T$ is the pulse repetition rate.

Because usually $\beta N_{e,max}^2(0)\gg\gamma_a$, expression (27) can be simplified:

$$\langle N_e(0,t)\rangle=\frac{f}{(\gamma_a\beta)^{1/2}}\arctan\left[\exp\left(\frac{2\gamma_a}{f}\right)-1\right]^{1/2}. \quad (28)$$

Since, according to (8),

$$n_e(0)=\frac{\langle N_e(0,t)\rangle}{N_{M,w}}, \quad (29)$$

$n_M^{(D)}(x)$ can be written in the form

$$n_M^{(D)}(x)=1-\sqrt{\xi}\left(\frac{f}{\beta N_{M,w}^2}\right)^{1/2}\left(\frac{f}{\gamma}\right)^{1/2}$$

$$\times\arctan\left[\exp\left(\frac{2\xi\gamma}{f}\right)-1\right]^{1/2}(1-x^2); \quad (30)$$

where we took into account that $\gamma_a=\xi\gamma$.

2.2 Thermal diffusion

The radial profile of the concentration $n_M^{(T)}(x)$ of metal atoms appearing due to the inhomogeneity of the gas temperature can be found from the heat conduction equation

$$\frac{1}{x}\frac{\mathrm{d}}{\mathrm{d}x}\left(x\lambda_{th}\frac{\mathrm{d}T_g}{\mathrm{d}x}\right)=-\frac{R^2wf}{e}, \quad (31)$$

where $w=W/V$ is the specific energy input; $e=1.6\times10^{-19}$ C is the electron charge; and

$$\lambda_{th}=AT_g^B \quad (32)$$

is the heat conductivity of the buffer gas.

For helium, $A=1.55\times10^{21}$ cm^{-1} s^{-1} eV^{-B}, where $B=0.787$ [11].

The temperature $T_g(x)$ should satisfy the boundary conditions

$$\frac{\mathrm{d}T_g(0)}{\mathrm{d}x}=0,\quad T_g(1)=T_w. \quad (33)$$

The solution of Eqn (31) satisfying conditions (33), under the second simplifying assumption, has the form

$$T_g(x)=\left[T_w^{B+1}+\frac{R^2wf(B+1)}{4eA}(1-x^2)\right]^{1/(B+1)}. \quad (34)$$

Therefore, according to (18), the radial profile caused by thermal diffusion is

$$n_M^{(T)}(x)=\left[1+\frac{R^2wf(B+1)}{4eAT_w^{B+1}}(1-x^2)\right]^{-1/(B+1)}. \quad (35)$$

2.3 Prepulse radial profile of the concentration of metal atoms

We consider the radial distribution of metal atoms averaged over the interpulse period. Because the current pulse duration in repetitively pulsed MVLs during which the plasma parameters drastically change is much shorter than the interpulse period, the averaged radial distribution of metal atoms will approximately coincide with their prepulse distribution.

By using (30) and (35), we represent the prepulse radial distribution of the concentration of metal atoms in the form

$$n_M(x)=\left[1+k_1(1-x^2)\right]^{-1/(B+1)}-(\xi k_2k_3)^{1/2}$$

$$\times\arctan\left[\exp\left(\frac{2\xi}{k_3}\right)-1\right]^{1/2}(1-x^2). \quad (36)$$

Here, the dimensionless parameters are introduced, which characterise the properties of a repetitively pulsed discharge:

$$k_1=\frac{R^2wf(B+1)}{4eAT_w^{B+1}} \quad (37)$$

is the ratio of the electric power supplied to the discharge to the thermal power released from it due to the heat conduction of the buffer gas;

$$k_2=\frac{f}{\beta N_{M,w}^2} \quad (38)$$

is the ratio of the pulse repetition rate to the maximum frequency of recombination (in this case, $N_{M,w}$ changes to N_e): and

$$k_3=\frac{f}{\gamma}=\frac{R^2}{6D}f \quad (39)$$

is the ratio of the pulse repetition rate to the diffusion frequency of metal atoms.

3. Calculations of radial distributions

To verify the applicability of expressions (30), (35), and (36) to real repetitively pulsed metal vapour lasers, we performed comparative calculations for eight different self-heating tubes of He–Sr lasers studied in papers [3–5, 9, 12–14]. The results of calculations obtained with the help of the detailed mathematical model of a He–Sr laser were used as the test results [15]. Figure 1 presents the results of calculations. Table 1 lists the laser parameters, the corresponding values of parameters k_1, k_2, and k_3, and the difference of concentrations of metal atoms on the tube wall and axis calculated from expressions (30), (35), and (36). Also, the values of ξ and T_e averaged over the interpulse period and calculated by using the model are presented.

One can see from Fig. 1 that calculations by expressions (30), (35), and (36) well agree with the results of detailed simulation of the plasma of the repetitively pulsed discharge of the He–Sr laser. In particular, good agreement is observed for the relative contributions of radial cataphoresis and thermal diffusion into the prepulse radial profile of the concentration of strontium atoms, the contribution from thermal diffusion being dominant for all the tubes. In all the cases, expression (30) gives a somewhat lower decrease in the concentration of metal atoms on the axis than the detailed calculation. This is explained by the fact that we derived expression (30) by assuming that the plasma contains only strontium ions, whereas it also contains helium ions, which make a small contribution to N_e. Some differences in thermal profiles calculated by (35) and with the help of the model are caused by small differences between the real energy supply to each tube and the homogeneous energy supply used in the derivation of (35).

The real distribution of the concentration of metal atoms along the tube radius can be called homogeneous only conditionally. In fact, as shown in Fig. 1, the radial profile $n_M(x)$ for repetitively pulsed MVLs is always inhomogeneous, at least due to the inhomogeneity of T_g, which will

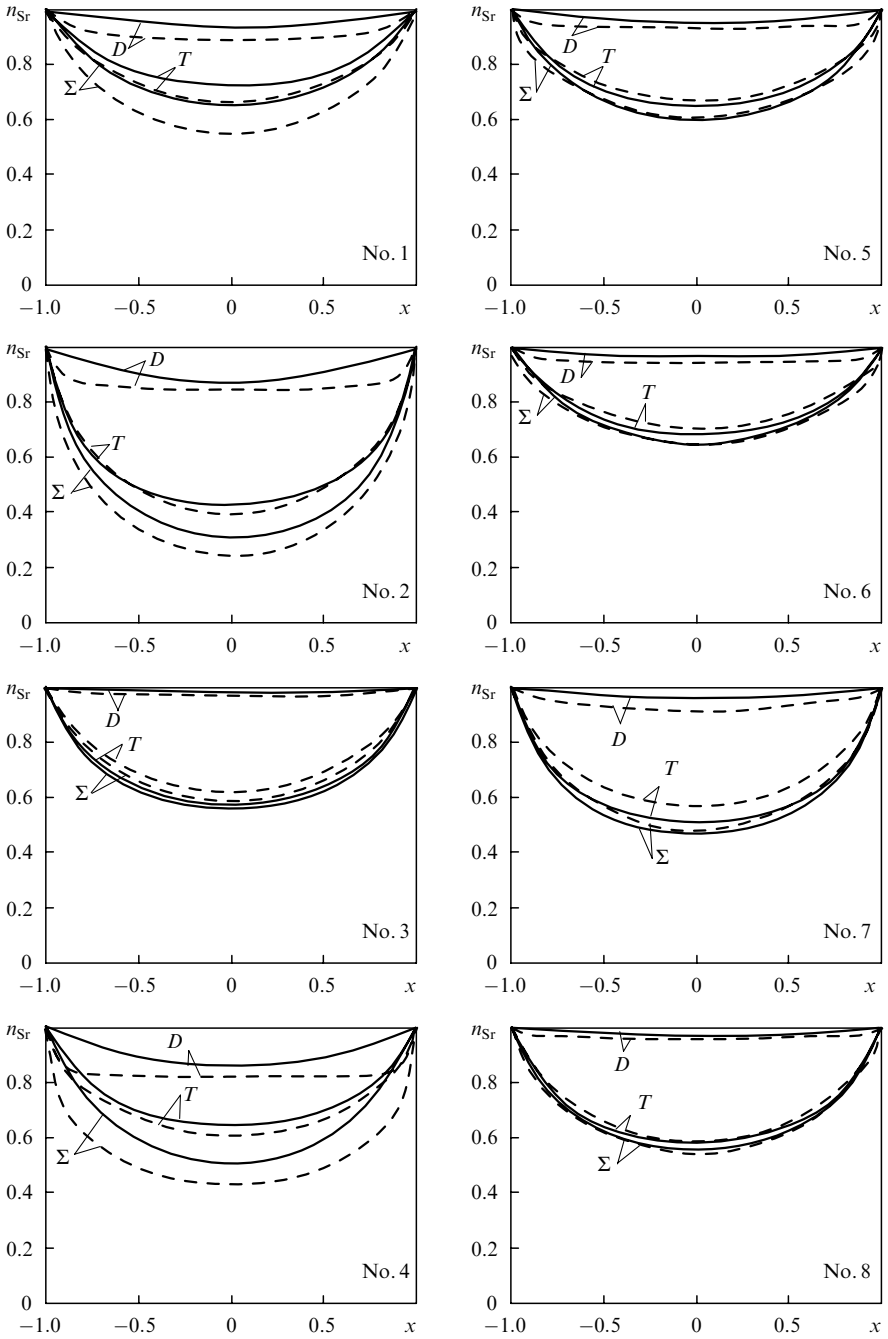

Figure 1. Comparison of the radial profiles of the concentration of strontium atoms calculated by expressions (30), (35), and (36) (solid curves) with profiles calculated by using the mathematical model of a He–Sr laser (dashed curves). Numbers in figures are the numbers of tubes in Table 1, the letters D and T indicate profiles caused by radial cataphoresis and thermal diffusion; Σ is the total profile.

Table 1. Parameters of the He–Sr lasers studied in papers [3–5, 9, 12–14], the corresponding values of k_1, k_2, and k_3, and the difference between concentrations on the tube wall and axis caused by radial cataphoresis [$\Delta n_M^{(D)}$] and thermal diffusion [$\Delta n_M^{(T)}$] calculated by expressions (30), (35), and (36); $\Sigma\Delta n_M$ is the total difference.

Tube number	References	R/cm	w/mJ	f/kHz	P_{He}/Torr	T_w/eV	$N_{Sr}(R)/10^{14}$ cm^{-3}	T_e/eV	ξ	k_1	$k_2/10^{-3}$	k_3	$\Delta n_M^{(D)}$(%)	$\Delta n_M^{(T)}$(%)	$\Sigma\Delta n_M$(%)
1	[9]	0.635	2.7	3.77	112	0.073	2.75	0.097	2.33	0.79	0.44	12.7	6.7	27.8	34.5
2	[12]	0.775	5.2	6	250	0.075	2	0.1	2.35	3.4	1.4	64.2	12.4	56.6	69.0
3	[13]	1.25	7.8	0.7	200	0.073	2.5	0.08	2.06	1.7	0.04	16.4	1.8	42.2	44.0
4	[3, 4]	0.15	21	30	608	0.075	6.7	0.12	2.62	2.3	0.17	106.6	14.2	35.5	49.7
5	[5, 14]	0.275	4.8	18	684	0.076	8.5	0.098	2.3	1.19	1.5	29.2	4.9	35.3	40.2
6	[5, 14]	0.3	5.9	10	608	0.076	7.5	0.09	2.2	1.17	0.23	65.2	3.2	31.5	34.7
7	[5, 14]	0.75	4.5	5	532	0.075	6.7	0.11	2.3	1.61	0.08	95.8	4.2	48.9	53.1
8	[5, 14]	0.5	4.5	8	684	0.076	6.7	0.084	2.1	0.96	0.01	38.6	2.7	41.6	44.3

have a maximum on the tube axis due to a finite heat conduction of the buffer gas, while the distribution of active particles will have a minimum.

A decrease in the concentration of metal atoms at the tube centre will affect the parameters of the laser. When the distribution has a deep minimum, the output power decreases noticeably, and the inhomogeneity of $n_M(x)$ becomes a decisive factor preventing the generation of high output powers from large volumes at high pulse repetition rates. In this case, the inhomogeneity of $n_M(x)$ leads to the inhomogeneities of the output parameters of MVLs, both on atomic [16] and ion transitions. In particular, in a He–Sr laser, where ion laser transitions are pumped due to the recombination of Sr^{++} ions, the radial distribution of the concentration of Sr^{++} under the conditions of almost complete double ionisation of Sr atoms almost completely repeats their prepulse radial distribution (except near-wall regions).

Let us use equality (36) to obtain the criterion for the homogeneity of the radial distribution of the concentration of metal atoms. It follows from (36) that the depth of the dip in the concentration of metal atoms on the axis is

$$\Delta n_M(0) = 1 - (1+k_1)^{-1/(B+1)} + (\xi k_2 k_3)^{1/2} \arctan\left[\exp\left(\frac{2\xi}{k_3}\right) - 1\right]^{1/2}. \quad (40)$$

One can see from Table 1 that the parameter ξ changes weakly depending on conditions: $\xi = 2 - 2.6$ (we will assume in estimates that $\xi = 2.3$). Consider the function

$$F(k_3) = (\xi k_3)^{1/2} \arctan\left[\exp\left(\frac{2\xi}{k_3}\right) - 1\right]^{1/2}, \quad (41)$$

whose plot is shown in Fig. 2. We assume in the plot that k_3 changes beginning from unity because it is accepted to treat the value γ_a as the lower frequency of a repetitively pulsed discharge [17]. It follows from Fig. 2 that for $k_3 > 10$, we can assume that $F(k_3) = 3.2$, i.e., the function is no longer dependent on k_3. One can see from Table 1 that the condition $k_3 > 10$ is fulfilled for all the tubes studied. Moreover, even for $k_3 < 10$, the replacement of $F(k_3)$ by the number 3.2 does not strongly affect the estimates. Therefore, we will assume that

$$\Delta n_M(0) = 1 - (1+k_1)^{-1/(B+1)} + 3.2\sqrt{k_2}. \quad (42)$$

As a criterion for the radial homogeneity of the concentration of metal atoms, we will use the condition

$$\Delta n_M(0) \leqslant \frac{2}{3} n_M(1) \approx 0.67, \quad (43)$$

which means that the depth $\Delta n_M(0)$ of the concentration dip of metal atoms on the axis should not exceed 2/3 of its value on the walls. The maximum admissible depth of the dip on the axis was selected by analysing the results of simulation of the He–Sr laser. We will call conditionally the distribution of metal atoms satisfying criterion (43) the homogeneous distribution. It follows from (42) that for the fulfilment of condition (43), the inequality

$$k_1 \leqslant \left(0.33 + 3.2\sqrt{k_2}\right)^{-(B+1)} - 1 \quad (44)$$

should be satisfied.

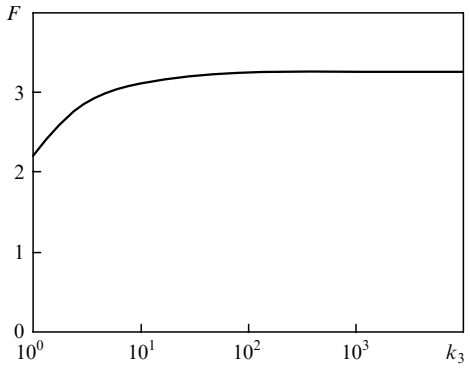

Figure 2. Plot of the function $F(k_3)$.

Condition (44), which is plotted in Fig. 3, means that for the radial homogeneity of the concentration of metal atoms to be homogeneous, the point (k_1, k_2), corresponding the laser parameters, should lie below or on the curve:

$$k_1 = \left(0.33 + 3.2\sqrt{k_2}\right)^{-(B+1)} - 1; \quad (45)$$

the region of the admissible values of (k_1, k_2) is indicated by grey. The numbers in Fig. 3 denote the points (k_1, k_2) corresponding to different tubes (see Table 1). Condition (44) is fulfilled for all the tubes except tube No. 2, which is

also seen from curves in Fig. 1. The point corresponding to tube No. 2 is located near the boundary of the region of admissible values of k_1 and k_2. This is explained by the fact that in this tube the strontium vapour is introduced independently during helium circulation, which allowed the authors [12] to increase the pulse repetition rate until the radial inhomogeneity of the metal vapour became substantial.

By substituting expressions (37) and (38) for k_1 and k_2 into (44), we obtain the criterion for the transverse homogeneity of active media of repetitively pulsed MVLs in the form

$$\left[0.33 + 3.2\left(\frac{f}{\beta N_{\mathrm{M,w}}^2}\right)^{1/2}\right]^{-(B+1)} - \frac{B+1}{4eA}\frac{R^2 wf}{T_{\mathrm{w}}^{B+1}} \geqslant 1. \quad (46)$$

The coefficients A and B for each buffer gas are constants, the value of β also can be considered approximately constant because the average value of T_{e} in the afterglow only weakly depends on conditions (see Tale 1). Therefore, inequality (46) imposes restrictions on the parameters R, w, f, T_{w}, and N_{w}. The ratio $f/(\beta N_{\mathrm{M,w}}^2)$ in the first term in the left side of (46) determines the depth of the dip of $n_{\mathrm{M}}(x)$ caused by radial cataphoresis. The greater f, the greater number of metal ions has time to leave the discharge due to ambipolar diffusion, thereby reducing the metal vapour content in the discharge, especially on the axis of the gas-discharge tube. The second term in the left side of (46) determines the depth of the dip in the radial metal vapour distribution caused by gas heating. The greater the product wf, i.e., the power supplied to the unit volume of the active medium, the higher the gas temperature on the axis and deeper the dip in the concentration of metal atoms. And the greater the tube radius R, the longer time of the energy release from the discharge, which also results in the increase in T_{g} on the axis and in the depth of the dip $n_{\mathrm{M}}(0)$.

One can see from Fig. 3 that condition (46) is fulfilled in most cases. However, it can be violated in some regimes (tube No. 2). The achievement of the spatial homogeneity of the active medium becomes especially important in large-volume lasers with a gas-discharge channel of large diameter. In this case, the problem of the radial inhomogeneity of metal vapours appears [13, 18–20]. One can see from (46) that the increase in R near curve (45) requires a drastic reduction of $f \propto 1/(wR^2)$ to preserve the spatial homogeneity of the active medium. In this case, the linear average output power will saturate:

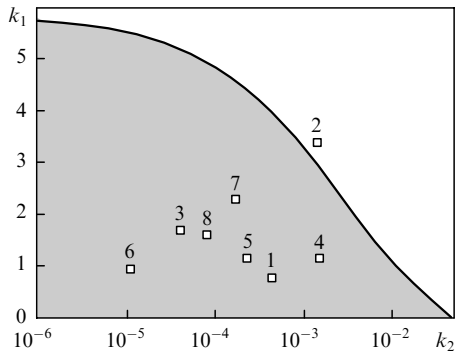

Figure 3. Region of the admissible values of parameters k_1 and k_2 corresponding to criterion (44).

$$\frac{P_{\mathrm{av}}}{L} = \frac{\eta w V}{L} f \propto \frac{\eta w \pi R^2 L}{L}\frac{1}{wR^2} \propto \eta \approx \mathrm{const}, \quad (47)$$

where η is the lasing efficiency. The pulse energy characteristics can achieve in this case high values. Thus, the pulse energy is $\varepsilon = \eta w V \propto \eta R^2$. For tubes of comparatively small diameter, when the spatial inhomogeneity of the active medium still does not affect lasing, the pulse repetition rate is determined by the heat removal conditions in the self-heating regime, $f \propto 1/(wR)$, while the linear output power increases with R as $P_{\mathrm{av}}/L \propto \eta R$ [14, 21]. Note that an increase in T_{g} (and T_{e}) on the axis in a He–Sr laser will be accompanied by a decrease in the recombination pump rate, resulting in a decrease in η and all energy characteristics. This factor, along with the formation of the spatial inhomogeneity of the active medium, also slows down an increase in energy characteristics with increasing R.

4. Optimal excitation regimes of cataphoresis repetitively pulsed MVLs

To build efficient cataphoresis repetitively pulsed lasers, it is necessary to provide simultaneously two conditions: to produce a homogeneous distribution of the metal vapour along the gas-discharge channel and ensure the degree of homogeneity of the metal vapour concentration along the tube radius which is sufficient for efficient lasing. As follows from [6, 7], to provide the first condition, the inequality

$$\frac{\theta E_0 L}{\langle T_{\mathrm{g}}\rangle} f\tau_{\mathrm{i}} \geqslant 10 \quad (48)$$

should be fulfilled. Here, E_0 is the initial field strength on a storage capacitor; θ is the ionisation degree of the metal vapour;

$$\langle T_{\mathrm{g}}\rangle = 2T_{\mathrm{w}}\int_0^1 \left[1 + k_1(1-x^2)\right]^{1/(B+1)} x\mathrm{d}x$$

$$= \frac{T_{\mathrm{w}}}{k_1}\frac{B+1}{B+2}\left[(1+k_1)^{(B+2)/(B+1)} - 1\right] \quad (49)$$

is the radius-averaged gas temperature obtained averaging (34);

$$\tau_{\mathrm{i}} = \zeta(L_{\mathrm{ind}}C)^{1/2} \quad (50)$$

is the current pulse duration; $\zeta \approx 4.25$ is the empirical coefficient; L_{ind} is the discharge circuit inductance, which can be calculated from the expression [11]

$$L_{\mathrm{ind}} = \left[2L\left(\ln\frac{2L}{R} - 1\right) + L_{\mathrm{ext}}\right] \times 10^{-9}\ \mathrm{H}; \quad (51)$$

and L_{ext} is the inductance of external circuits, which is usually ~ 0.5 μH. To provide the second condition, inequality (46) should be fulfilled.

Thus, we have two conditions imposing restrictions on the excitation parameters of cataphoresis repetitively pulsed MVLs. For example, to provide the efficient vapour circulation by cataphoresis and produce the homogeneous distribution of active particles over the tube length, it is necessary, as follows from (48), to increase the pulse repetition rate f, but condition (46) limits its value from

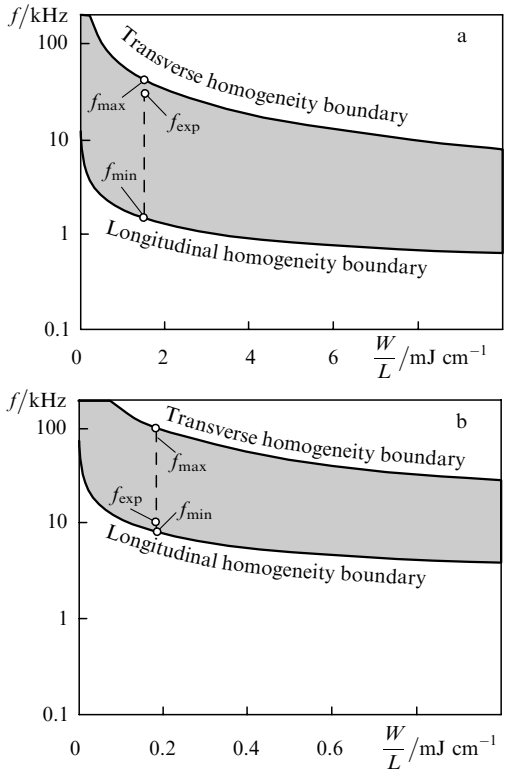

Figure 4. Regions of the admissible values of W/L and f for the He–Sr (a) and He–Cd (b) lasers studied in [3, 4] (grey regions); the vertical dashed straight lines indicate the frequency ranges satisfying conditions (46) and (48) for the linear energy input used in papers [3, 4] (for the He–Sr, $W/L = 1.52$ mJ cm^{-1}, $f_{min} = 1.5$ kHz, $f_{max} = 42$ kHz, $f_{exp} = 30$ kHz; for the He–Cd laser, $W/L = 0.18$ mJ cm^{-1}; $f_{min} = 8.3$ kHz, $f_{max} = 100$ kHz, $f_{exp} = 10$ kHz).

above due to the decrease in the metal concentration at the tube centre caused by its thermal diffusion and radial cataphoresis to the tube walls.

By using (46) and (48), we can calculate the upper and lower boundaries of the region of optimal excitation parameters for repetitively pulsed MVLs, which provide a high degree of homogeneity of their active media. These boundaries are shown in Fig. 4a for the He–Sr laser and Fig. 4b for the He–Cd laser. One can see that excitation regimes for both lasers realised in [3, 4] are in the range of optimal parameters. In particular, the He–Sr laser operated at the pulse repetition rate $f_{exp} = 30$ kHz [3, 4], which is close (Fig. 4a) to the maximum possible rate $f_{max} = 42$ kHz, which is admissible, according to (46), for the linear energy input $W/L = 1.52$ mJ cm^{-1}. In this case, the criterion for the longitudinal homogeneity (48) is fulfilled with a great safety margin because $f_{min} = 1.5$ kHz. It follows from Fig. 4b that the repetitively pulsed cataphoresis He–Cd laser [3, 4] also operated in the region of optimal parameters ($f_{exp} = 10$ kHz, $W/L = 0.18$ mJ cm^{-1}) and had a substantial safety margin in the rate f.

5. Conclusions

We have studied the mechanisms of formation of the radial profile of the concentration of metal vapours in repetitively pulsed MVLs. It has been shown that overheating of the axial regions of the discharge and radial cataphoresis produce the deficit of active particles at the laser tube centre, which can impair the output characteristics of the laser. The criterion has been obtained whose fulfilment ensures the concentration of metal vapours on the tube axis amounting to no less than 1/3 of its value on the tube walls. This condition is valid both for cataphoresis and conventional repetitively pulsed MVLs. These results are confirmed by calculations based on the detailed mathematical model of a recombination He–Sr laser.

It has been shown that for cataphoresis repetitively pulsed MVLs the criteria for the longitudinal and radial homogeneity of the concentration of metal vapours should be fulfilled simultaneously. The boundaries of the region of optimal excitation parameters of active media providing a high degree of their homogeneity are determined.

The results obtained in the paper allow the purposeful selection of excitation regimes providing a high degree of homogeneity of the active media of repetitively pulsed MVLs and, therefore, their efficient output parameters.

Acknowledgements. This work was supported by the Russian Foundation for Basic Research (Grant No. 04-02-96804).

References

1. Ivanov I.G., Latush E.L., Sem M.F. *Ionnnye lazery na parakh metallov* (Ion Metal Vapour Lasers) (Moscow: Energoatomizdat, 1990).
2. Little C.E. *Metal Vapour Lasers: Physics, Engineering and Applications* (Chichester, New York: John Willey & Sons, 1999).
3. Latush E.L., Chebotarev G.D., Vasil'chenko A.V. *Opt. Atmos. Okean.*, **11**, 171 (1998).
4. Latush E.L., Chebotarev G.D., Vasilchenko A.V. *Proc. SPIE Int. Soc. Opt. Eng.*, **3403**, 141 (1998).
5. Latush E.L., Chebotarev G.D., Sem M.F. *Kvantovaya Elektron.*, **30**, 471 (2000) [*Quantum Electron.*, **30**, 471 (2000)].
6. Chebotarev G.D., Prutsakov O.O., Latush E.L. *Opt. Atmos. Okean.*, **14**, 1011 (2001).
7. Chebotarev G.D., Prutsakov O.O., Latush E.L. *Proc. SPIE Int. Soc. Opt. Eng.*, **4747**, 187 (2002).
8. Redko T.P., Kosinar I. *Czech. J. Phys. B*, **30**, 1293 (1980).
9. Kunnemeyer R., McLucas C.W., Brown D.J.W., McIntosh A.I. *IEEE J. Quantum Electron.*, **23** (11), 2028 (1987).
10. Veselovskii I.S. *Zh. Tekh. Fiz.*, **39**, 271 (1969).
11. Batenin V.M., Buchanov V.V., Kazaryan M.A., Klimovskii I.I., Molodykh E.I. *Lazery na samoogranichennykh perekhodakh atomov metallov* (Self-Terminated Metal Atomic Transition Lasers) (Moscow: Nauchnaya Kniga, 1998).
12. Loveland D.G., Webb C.E. *J. Phys. D: Appl. Phys.*, **25**, 597 (1992).
13. Little C.E., Piper J.A. *IEEE J. Quantum Electron.*, **26** (5), 903 (1990).
14. Chebotarev G.D., Latush E.L. *Kvantovaya Elektron.*, **30**, 393 (2000) [*Quantum Electron.*, **30**, 393 (2000)].
15. Chebotarev G.D., Prutsakov O.O., Latush E.L. *Abstracts of Papers, Simpozium 'Lazery na parakh metallov'* (Symposium on Metal Vapour Lasers) (Rostov-on-Don, 2004) p. 24.
16. Soldatov A.N., Shaparev N.Ya., Kirilov A.E., Glizer V.Ya., Plunin Yu.P., Fedorov V.F. *Izv. Vyssh. Uchebn. Zaved., Ser. Fiz.*, (10), 38 (1980).
17. Klimkin V.M. *Preprint Inst. Opt. Atmos., Siberian Branch, RAS*, (1) (Tomsk, 1999).
18. Butler M.S., Piper J.A. *IEEE J. Quantum Electron.*, **21** (10), 1563 (1985).
19. Little C.E., Piper J.A. *Opt. Commun.*, **68** (4), 282 (1988).
20. Little C.E., Piper J.A. *Proc. SPIE Int. Soc. Opt. Eng.*, **1041**, 167 (1989).
21. Chebotarev G.D., Latush E.L., Sotnikov R.Yu. *J. Moscow Phys. Soc.*, (7), 129 (1997).